Design of a High-Gain Wideband Co-Planar Waveguide Antenna for Wireless Communications Using Metamaterial Techniques

Narayanarao Potnuru

Department of ECE, Aditya Institute of Technology and Management, Tekkali, AP-532201, India narayana1student@gmail.com (corresponding author)

Karunakar Godi

Department of ECE, GITAM (Deemed to be University), Visakhapatnam, AP-530045, India kgodi@gitam.edu

Received: 18 April 2025 | Revised: 22 May 2025 | Accepted: 31 May 2025

Licensed under a CC-BY 4.0 license | Copyright (c) by the authors | DOI: https://doi.org/10.48084/etasr.11565

ABSTRACT

This study presents the design and analysis of a compact metamaterial-based antenna, tailored for wideband wireless communication systems and intended primarily for commercial use. The antenna combines a Co-planar Waveguide (CPW) structure with a Square Ring Resonator (SRR), aiming to boost both bandwidth and gain. Fabricated on a standard FR4 substrate with overall dimensions of $24 \times 24 \times 1.6$ mm³, the antenna's performance was first optimized using CST Microwave Studio, a full-wave Electromagnetic (EM) simulation platform. Key parameters, such as the reflection coefficient (S11), radiation pattern, and gain were thoroughly evaluated. The simulation predicted a wide operating bandwidth of 7 GHz, ranging from 2.8 to 9.8 GHz, with a peak gain of 4.7 dBi. Following fabrication via photolithography, an experimental validation was carried out using a Vector Network Analyzer (VNA). The measured results demonstrated excellent agreement with the simulations, revealing an even broader bandwidth of approximately 8.2 GHz (1.58–9.8 GHz) and a slightly improved peak gain of approximately 5.14 db. These findings confirm the reliability of the proposed design and underline its potential as a practical solution for modern wideband wireless applications.

Keywords- CPW; SRR; CST; metamaterials; bandwidth

I. INTRODUCTION

Metamaterial antennas have attracted significant interest. These structures can manipulate the EM waves in ways that conventional materials cannot. They offer unique properties, such as negative permittivity and permeability. As a result, they support enhanced performance, including multiband and wideband operation [1-3]. Research focuses on integrating resonant elements, like Split-Ring Resonators (SRRs) and Complementary SRRs (CSRRs). These elements allow designers to tune resonance across specific frequency bands [4]. Other approaches include mushroom-like structures and high-impedance surfaces. These have improved the bandwidth and radiation efficiency, especially for Ultra-Wideband (UWB), radar, and 5G applications [5].

Metamaterials are also used in MIMO antennas. Superstrates, for example, improve gain and isolation [6]. Techniques, such as the Electromagnetic Bandgap (EBG) and Defected Ground Structures (DGS), help reduce the mutual

coupling in dense arrays [7]. Circularly polarized antennas using parasitic elements have also shown a promising wideband performance.

Advances in the metamaterial-based antenna design have significantly improved the performance of multiband and MIMO systems. In [8], fractal antennas enhanced with metamaterial structures are shown to achieve UWB performance while reducing the mutual coupling and maintaining a compact size. Authors in [9] apply hybrid metamaterial techniques to improve isolation in MIMO systems improving the Electromagnetic Interference (EMI). In [10], a wideband circularly polarized Microstrip Patch Antenna (MPA) with enhanced gain is presented.

Authors in [11] introduce the use of CRLH metamaterial cells for triple-band and multiband monopole antennas. Dualband antennas with asymmetric hybrid resonators are designed in [12], achieving extremely compact structures. The enhancement of gain and reduction of Synthetic Aperture

Radar (SAR) in wearable devices through metamaterial slabs is explored in [13]. Characteristic Mode Analysis (CMA) with a superstrate is applied in [14] to optimize the array performance. Metamaterials and DGS are utilized in [15, 16] to design compact, high-gain patch antennas. In [17], compact and directive 5G mm-wave antenna is demonstrated, using a meta surface derived from the Luneburg lens concept.

The current work builds on these advancements by proposing a compact metamaterial antenna with a wide bandwidth and high gain, suitable for modern wireless communication systems.

II. PROPOSED ANTENNA GEOMETRY WITH SRR METAMATERIAL

The geometry of the proposed antenna is illustrated in Figures 1(a) and 1(b), demonstrating the CPW-based U-slot radiator and the integrated metamaterial structure, respectively. The antenna is fabricated on an FR4 substrate with a relative permittivity (ε_r) of 4.4. Its overall dimensions are $24\times24\times1.6$ mm³. The radiating element follows a U-slot configuration, while the ground plane features two inverted arc-shaped stubs extending into the slot region.

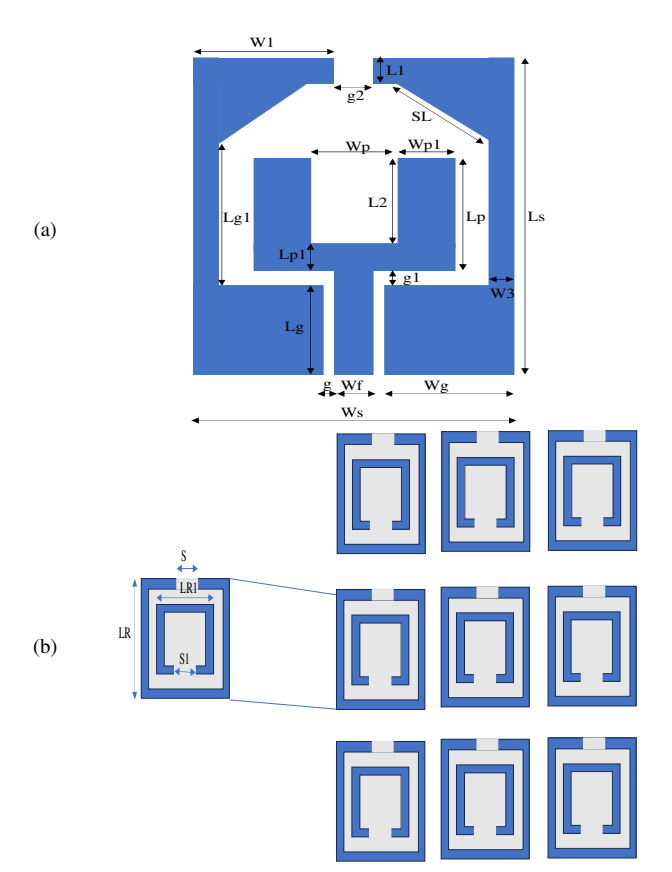


Fig. 1. Proposed antenna: (a) geometry and (b) metamaterial model.

A CPW feed system is implemented using a central strip line flanked by two gaps, directing the energy toward the slot region. The ground plane consists of two symmetrical metallic sections that run around the slot, within the square substrate boundary. The CPW feed offers several advantages, including low dispersion, reduced radiation loss, ease of integration with active devices, and simplified fabrication. Two inverted arc shaped stubs are placed back-to-back, extending from the ends of a T-shaped microstrip feed line, and are separated by a defined gap. The SRR-based metamaterial structure is shown in Figure 1(b). The dimensions of both the antenna and the SRR unit cell are listed in Table I. A 3×3 array of SRRs is positioned above the antenna structure, as depicted in Figure 1(a), at a vertical distance of 5 mm.

TABLE I. DESIGN PARAMETERS OF THE PROPOSED ANTENNA

No.	Parameter	Value (mm)		
1	Ws	24		
2	Ls	24		
3	Wf	3		
4	Lf	2.9		
5	Lp1 Wp	2		
6	Wp	5		
7	Wp1	4.5		
8	gl	0.2		
9	Lp	9		
10	g	0.55		
11	Wg Lg WI	10		
12	Lg	8.5		
13	W1	11.5		
14	LI	2		
15	G2	1		
16	L2	7		
17	SL	5		
18	W3	1		

The proposed antenna configuration contributes to the wideband performance by optimizing the impedance matching and radiation characteristics.

III. SIMULATION RESULTS

The proposed antenna geometry was simulated using CST Microwave Studio, a commercially available 3D full-wave EM solver. CST provides a CAD-based interface and solves Maxwell's equations using the Method of Moments (MoM), which is suitable for analysing complex EM structures with high accuracy. The CPW-based U-slot antenna was modeled with the appropriate boundary conditions. Excitation was applied at the edge of the CPW feed using a wave port. The simulation domain was meshed with a 5×5 mm grid. Built-in optimization tools were used to refine the antenna structure, particularly for feed dimensions, which are often challenging in irregular geometries. The key design parameters include the feed gap (g), U-slot length (L_2) , patch length (Lp), ground length (Lg), and feed length (Lf). The optimized values produced stable results across the desired frequency band. The simulated S-parameter results, shown in Figure 2, indicate a wide impedance bandwidth of 7 GHz (2.8-9.8 GHz). The presence of the metamaterial layer introduces multiple resonances, contributing to wideband behavior. The gap g between the feed line and ground was varied from 0.4 to 0.6 mm in 0.1 mm steps. As depicted in Figure 2(a), the return loss stayed below -10 dB across 2.8–9.8 GHz. The U-slot length L_2 was swept from 6.5 to 7.5 mm in 0.5 mm steps. Figure 2(b) displays its effect on the impedance matching, confirming that L_2 controls the resonant response.

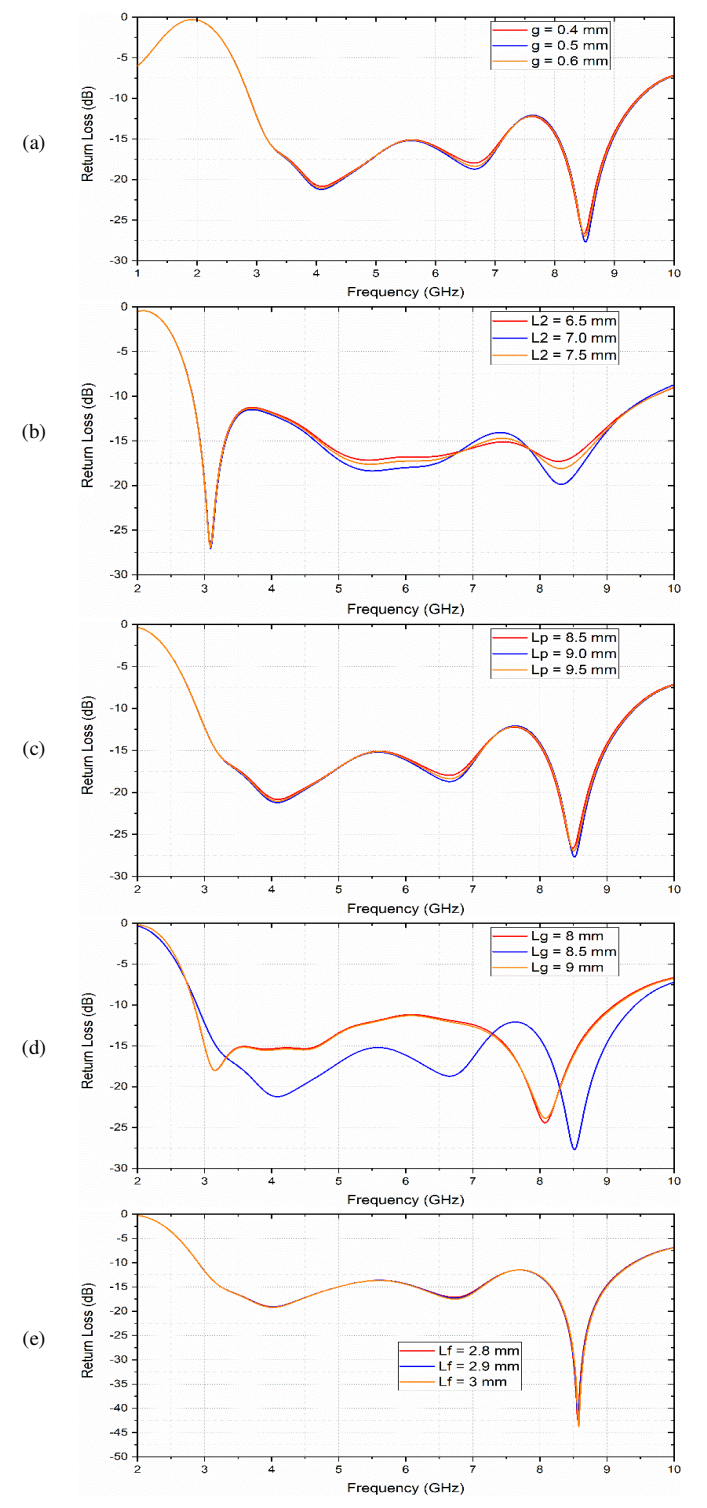


Fig. 2. Simulation results of the proposed antenna by varying the parameters: (a) g, (b) L2, (c) Lp, (d) Lg, and (e) Lf.

The parametric simulation results for the patch length (Lp), ground length (Lg), and feed length (Lf) are illustrated in Figures 2(c, d, e). All configurations satisfy the bandwidth and return loss requirements, confirming the robustness of the design.

The 2D and 3D radiation characteristics of the proposed antenna are depicted in Figures 3 and 4, respectively. Figure 3 presents the 2D radiation patterns at four representative frequencies: 3.1 GHz, 5.1 GHz, 7.5 GHz, and 8.5 GHz. At each frequency, the antenna exhibits a stable directional radiation behavior. The main lobe is oriented toward the patch side, indicating an effective forward radiation, while the radiation toward the ground plane side remains minimal, as expected.

This pattern confirms that the antenna maintains a good directivity and radiation efficiency throughout the operating band. The shape and symmetry of the lobes also suggest a consistent performance and minimal distortion at higher frequencies, which is critical for wideband wireless communication systems.

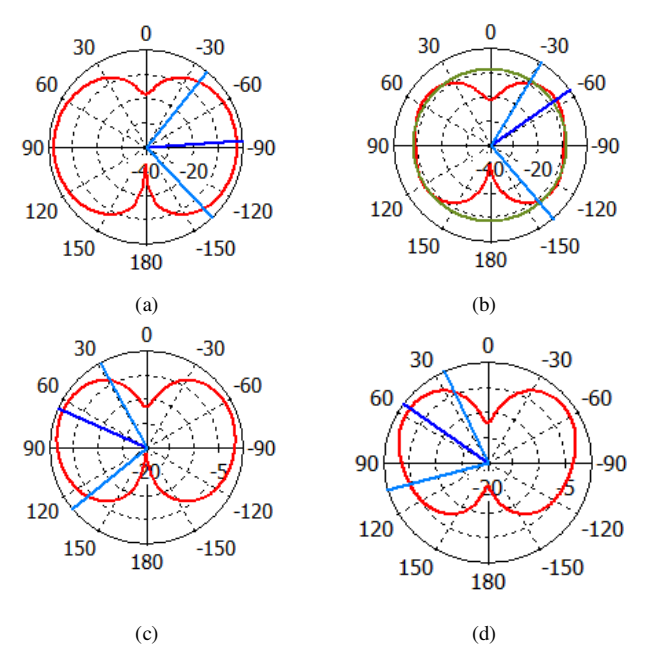


Fig. 3. 2D radiation patterns of the proposed antenna without metamaterial at: (a) 3.1~GHz, (b) 5.1~GHz, (c) 7.5~GHz, and (d) 8.5~GHz.

The 3D radiation patterns of the proposed CPW antenna are shown in Figure 4. The results at 3.1, 5.1, 7.5, and 8.5 GHz are presented in Figure 4(a, b, c, d), respectively. The radiation characteristics of the proposed antenna are summarized in Table II. Parameters, such as the beamwidth and gain, are listed for the frequencies of 3.1, 5.1, 7.5, and 8.5 GHz. The proposed antenna integrated with the metamaterial structure is shown in Figure 1(b). The corresponding 2D radiation patterns are presented in Figure 5. Figures 5(a, b, c, d) illustrate the patterns at 3.1, 5.1, 7.5, and 8.5 GHz, respectively.

TABLE II. MEASURED RADIATION PARAMETERS OF THE CPW ANTENNA WITHOUT METAMATERIAL

No.	Frequency (GHz)	Beamwidth (deg)	Gain (dBi)
1	3.1	94.1	2.01
2	5.1	100.3	3.05
3	7.5	100.9	3.45
4	8.5	81.1	3.9

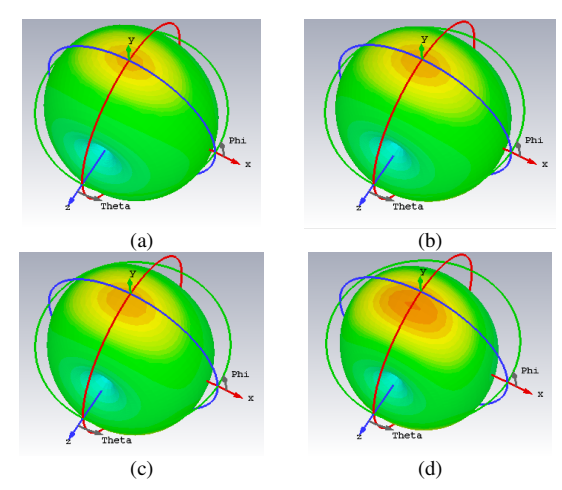


Fig. 4. 3D radiation patterns of the proposed antenna without metamaterial at: (a) 3.1 GHz, (b) 5.1 GHz, (c) 7.5 GHz, and (d) 8.5 GHz.

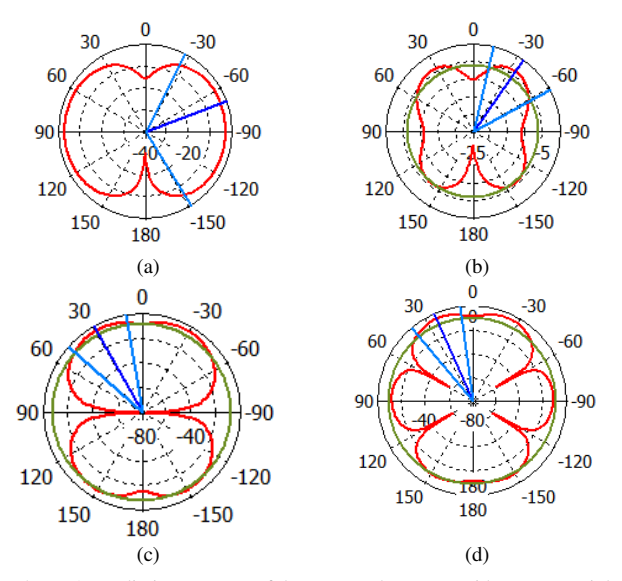


Fig. 5. 2D radiation patterns of the proposed antenna with metamaterial at: (a) 3.1 GHz, (b) 5.1 GHz, (c) 7.5 GHz, and (d) 8.5 GHz.

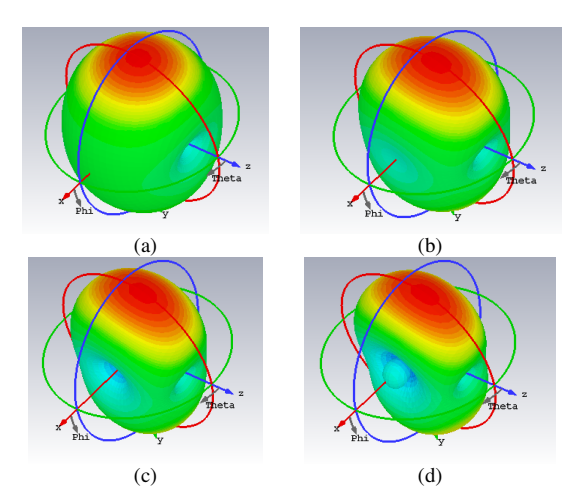


Fig. 6. 3D radiation patterns of the proposed metamaterial-based antenna at: (a) 3.1 GHz, (b) 5.1 GHz, (c) 7.5 GHz, and (d) 8.5 GHz.

The 3D radiation pattern of the proposed metamaterial-based antenna is portrayed in Figure 6, confirming a consistent directional behavior across the tested frequencies.

The 3D radiation patterns indicate the maximum power in red, aligned with the main radiation direction. The CPW feed provides a symmetric radiation with low cross-polarization. The metamaterial structure enables multiple resonant bands and maintains a stable radiation across the wide operating bandwidth.

The radiation characteristics of the proposed metamaterial-based CPW antenna are listed in Table III. The beamwidth and gain values for 3.1, 5.1, 7.5, and 8.5 GHz are provided.

TABLE III. BEAMWIDTH AND GAIN OF THE ANTENNA WITH METAMATERIAL

No.	Frequency	Beamwidth	Gain
	(GHz)	(deg)	(dBi)
1	3.1	120.0	3.08
2	5.1	60.2	4.39
3	7.5	58.5	4.85
4	8.5	62.3	5.09

The simulation results show that the gain and beamwidth of the metamaterial-based antenna are improved compared to the CPW antenna without metamaterial.

IV. EXPERIMENTAL RESULTS AND VALIDATION

The fabricated prototypes of the CPW antenna and the 3×3 SRR metamaterial structure are illustrated in Figures 7(a) and 7(b), respectively. The integrated metamaterial-based CPW antenna is presented in Figure 7(c). Fabrication was performed using standard photolithography techniques. The measurements were conducted using a Keysight VNA, and the corresponding return loss results are depicted in Figure 8.

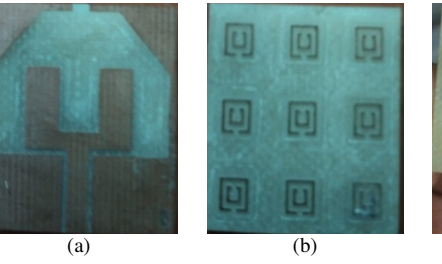




Fig. 7. Fabricated prototype of proposed antenna: (a) CPW based antenna, (b) metamaterial structure, and (c) metamaterial with CPW antenna.

The measured results exhibit a return loss below 10 dB over the 1.58–9.8 GHz range, corresponding to an 8.2 GHz bandwidth, as presented in Figure 8. This improvement is attributed to better impedance matching.

The measured radiation patterns of the proposed metamaterial-based CPW antenna are displayed in Figure 9. Figures 9(a, b, c) show the E-plane and H-plane patterns at 3.1, 7.5, and 8.5 GHz, respectively. The results demonstrate a consistent radiation behavior across the tested frequencies, confirming the stability of the antenna's performance within the wide operating band.

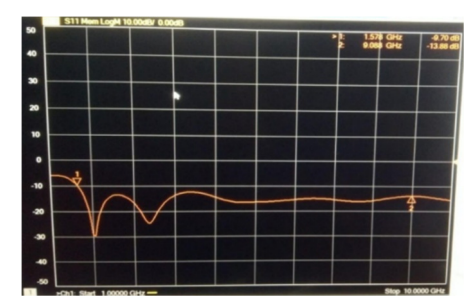


Fig. 8. Measured S11 of the fabricated antenna prototype.

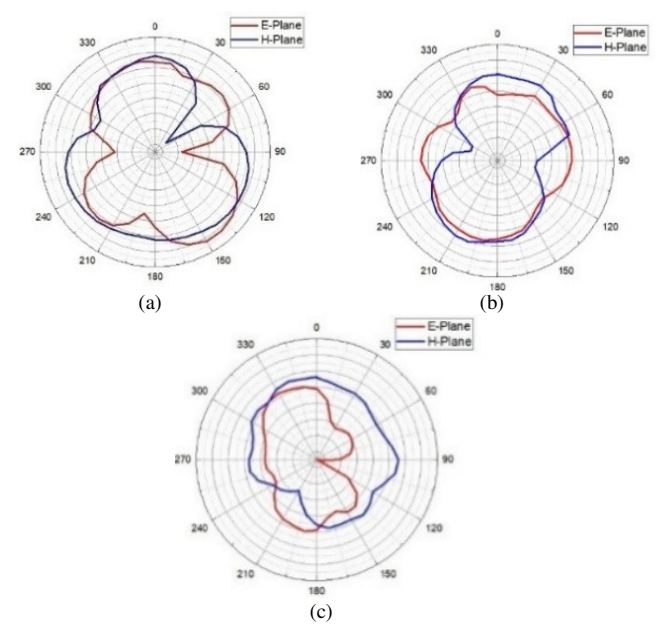


Fig. 9. Measured E-plane and H-plane radiation patterns of the proposed antenna with metamaterial at: (a) 3.1 GHz, (b) 7.5 GHz, and (c) 8.5 GHz.

The radiation characteristics of the proposed metamaterialbased CPW antenna are summarized in Table IV. The measured beamwidth and gain values are presented at multiple frequencies within the antenna's operating band. These values are compared with the corresponding simulation results and exhibit strong agreement across all tested frequencies. This consistency between the measured and simulated data validates the accuracy of the design and confirms the reliable performance of the antenna under practical conditions.

TABLE IV. MEASURED RADIATION CHARACTERITSTICS OF THE PROPOSED ANTENNA WITH METAMATERIAL

No.	Frequency (GHz)	Beamwidth (deg)	Gain (dBi)
1	3.1	118	3.12
2	7.5	62	4.75
3	8.5	64	5.14

Table V further compares the proposed CPW antenna with existing designs in terms of the operating frequency, bandwidth, physical size, gain, substrate properties, and the implemented metamaterial structure. The comparison highlights that the proposed antenna achieves an improved performance across multiple parameters. Specifically, it offers a wider bandwidth and higher gain, while maintaining compact dimensions and utilizing a standard low cost FR4 substrate. These results confirm that the proposed design is more efficient than the existing approaches, making it suitable for high-gain, wideband wireless communication applications.

V. CONCLUSION

The proposed metamaterial-based Co-planar Waveguide (CPW) antenna demonstrates excellent performance in terms of bandwidth and gain, making it a strong candidate for wideband wireless communication applications. The integration of a Split-Ring Resonator (SRR) with the CPW structure enhances the antenna's operational characteristics, resulting in a simulated bandwidth of 7 GHz and a measured bandwidth of approximately 8.2 GHz. The corresponding peak gains are 4.7 dBi and 5.14 dBi, respectively.

TABLE V. COMPARATIVE ANALYSIS OF THE PROPOSED ANTENNA AND REPORTED DESIGNS

Reference	Operating frequency (GHz)	BW (GHz)	Size (mm³)	Gain (dB)	Dielectric constant	Metamaterial structure type
[8]	2.3-2.5, 3.3-3.8, 5.3-5.9	0.2, 0.5, 0.6	35x32x1.6	0, 1.6, 2.7	4.4	CRLH cells
[9]	2.15-3.3, 5.51-7.25	1.15, 1.75	19.8x10x3	2.23, 5.72	2.65	Complementary spiral resonators
[10]	2.2-2.6, 3.4-3.6, 5-6.9	0.4, 0.2, 1.9	20x13x1.6	2.7, 3	4.4	SRR loaded MTM
[11]	5.5-6.1	0.6	13.27x27.5x2	7.9	2.7	CMA and Meta surface
[12]	3.451-3.524	0.073	50x50x1.52	6.3	3	Triangular MTM patch antenna
[13]	10.285-10.753	0.468	39x30	6.2	3.75	Metamaterial using DGS
[14]	2.35-2.58	0.227	-	6.511	4.4	Suspended hexagonal MPA
[15]	2.4-5.8	3.2	180x90	~6	4.4	Metamaterial MPA
[16]	2.55-2.72	0.17	105x72.5x1.58	15.8	4.4	Multilayer metamaterial
[18]	1.63-4.88	3.25	70x70x1.6	4.5	4.4	SRR Metamaterial
[19]	2.1-5.6	3.5	48x48x1.6	4.7	4.4	SRR
Proposed work	1.58-9.8	8.22	24x24x1.6	5.14	4.4	SRR

The close agreement between the simulated and measured results confirms the reliability of the design approach and the accuracy of the fabrication process. Due to its compact size, wide impedance bandwidth, and high radiation efficiency, the

antenna is well-suited for commercial wireless systems requiring stable and efficient wideband performance.

REFERENCES

- [1] A. Alu, N. Engheta, A. Erentok, and R. W. Ziolkowski, "Single-Negative, Double-Negative, and Low-index Metamaterials and their Electromagnetic Applications," *IEEE Antennas and Propagation Magazine*, vol. 49, no. 1, pp. 23–36, Oct. 2007, https://doi.org/10.1109/MAP.2007.370979.
- [2] V. G. Veselago, "THE ELECTRODYNAMICS OF SUBSTANCES WITH SIMULTANEOUSLY NEGATIVE VALUES OF AND µ," Soviet Physics Uspekhi, vol. 10, no. 4, Apr. 1968, Art. no. 509, https://doi.org/10.1070/PU1968v010n04ABEH003699.
- [3] J. B. Pendry, A. J. Holden, W. J. Stewart, and I. Youngs, "Extremely Low Frequency Plasmons in Metallic Mesostructures," *Physical Review Letters*, vol. 76, no. 25, pp. 4773–4776, Jun. 1996, https://doi.org/10.1103/PhysRevLett.76.4773.
- [4] A. Marwaha, "An Accurate Approach of Mathematical Modeling of SRR and SR for Metamaterials," *Journal of Engineering Science and Technology Review*, vol. 9, no. 6, pp. 82-86, Dec. 2016, https://doi.org/10.25103/jestr.096.11.
- [5] W. Liu, Z. N. Chen, and X. Qing, "Low-profile broadband antennas using metamaterial-mushroom structures," in 2015 IEEE International Conference on Computational Electromagnetics, Hong Kong, China, 2015, pp. 33-34, https://doi.org/10.1109/COMPEM.2015.7052545.
- [6] B. A. F. Esmail and S. Koziel, "Design and Optimization of Metamaterial-Based Dual-Band 28/38 GHz 5G MIMO Antenna With Modified Ground for Isolation and Bandwidth Improvement," *IEEE Antennas and Wireless Propagation Letters*, vol. 22, pp. 1069–1073, May. 2023, https://doi.org/10.1109/LAWP.2022.3232622.
- [7] C. Milias et al., "Metamaterial-Inspired Antennas: A Review of the State of the Art and Future Design Challenges," *IEEE Access*, vol. 9, pp. 89846–89865, 2021, https://doi.org/10.1109/ACCESS.2021.3091479.
- [8] M. H. Reddy, D. Sheela, V. K. Parbot, and A. Sharma, "A compact metamaterial inspired UWB-MIMO fractal antenna with reduced mutual coupling," *Microsystem Technologies*, vol. 27, no. 5, pp. 1971–1983, May 2021, https://doi.org/10.1007/s00542-020-05024-z.
- [9] M. Ameen and R. K. Chaudhary, "Isolation Enhancement of Metamaterial-Inspired Two-Port MIMO Antenna Using Hybrid Techniques," *IEEE Transactions on Circuits and Systems II: Express Briefs*, vol. 70, no. 6, pp. 1966–1970, Jun. 2023, https://doi.org/10.1109/TCSII.2023.3237831.
- [10] A. Kumar, S. Dwari, G. P. Pandey, B. K. Kanaujia, and D. K. Singh, "A high gain wideband circularly polarized microstrip antenna," *International Journal of Microwave and Wireless Technologies*, vol. 12, no. 7, pp. 678–687, Sep. 2020, https://doi.org/10.1017/S1759078719001612.
- [11] M. A. Abdalla, Z. Hu, and C. Muvianto, "Analysis and design of a triple band metamaterial simplified CRLH cells loaded monopole antenna," *International Journal of Microwave and Wireless Technologies*, vol. 9, no. 4, pp. 903–913, May 2017, https://doi.org/10.1017/S1759078716000738.
- [12] J.-X. Zhu, P. Bai, and J.-F. Wang, "Ultrasmall Dual-Band Metamaterial Antennas Based on Asymmetrical Hybrid Resonators," *International Journal of Antennas and Propagation*, vol. 2016, no. 1, 2016, Art. no. 7019268, https://doi.org/10.1155/2016/7019268.
- [13] S. Rosaline, "A triple-band antenna with a metamaterial slab for gain enhancement and specific absorption rate (Sar) reduction," *Progress In Electromagnetics Research C*, vol. 109, pp. 275–287, Jan. 2021, https://doi.org/10.2528/PIERC20122202.
- [14] K. D. Bhavani, B. T. P. Madhav, S. Das, N. Hussain, S. S. Ali, and K. V. Babu, "Development of Metamaterial Inspired Non-Uniform Circular Array Superstate Antenna Using Characteristic Mode Analysis," *Electronics*, vol. 11, no. 16, Jan. 2022, Art. no. 2517, https://doi.org/10.3390/electronics11162517.
- [15] G. Dai, X. Xu, and X. Deng, "Size-Reduced Equilateral Triangular Metamaterial Patch Antenna Designed for Mobile Communications," *Applied Computational Electromagnetics Society Journal (ACES)*, vol. 36, no. 8, Aug. 2021, https://doi.org/10.47037/2021.ACES.J.360811.
- [16] L. C. Paul, Md. A. Haque, S. Sarker, Md. M. Ur Rashid, Md. A. Haque, and T. K. Roy, "Design and Performance Exploration of a DGS

- Metamaterial MPA by Etching Four Dual Isosceles Triangular Defects on the Ground Plane," in 2018 International Conference on Computer, Communication, Chemical, Material and Electronic Engineering (IC4ME2), Rajshahi, Bangladesh, 2018, pp. 1-4, https://doi.org/10.1109/IC4ME2.2018.8465670.
- [17] K. C. Rao, D. Nataraj, K. S. Chakradhar, G. V. Ujwala, M. Lakshmunaidu, and H. S. Dadi, "Design of a Compact Millimeter Wave Antenna for 5G Applications based on Meta Surface Luneburg Lens," *Engineering, Technology & Applied Science Research*, vol. 15, no. 2, pp. 20722–20728, Apr. 2025, https://doi.org/10.48084/etasr.9349.
- [18] K. Rathod, Md. M. Bhakar, M. S. Mathpati, S. R. Chougule, and R. G. Sonkamble, "Bandwidth Improvement of Multilayer Microstrip Patch Antenna by Using Capacitive Feed Technique for Broadband Application," in *Techno-Societal* 2020, London, UK: Springer Nature, pp. 23–30, https://doi.org/10.1007/978-3-030-69921-5_3..
- [19] P. Narayanarao and G. Karunakar, "Compact High Gain Wide Band Planar Antenna Design Using Metamaterial Techniques For Wireless Applications," *International Journal of Computing and Digital Systems*, vol. 18, no. 1, pp. 1–14, Apr. 2025, http://doi.org/10.12785/ijcds/1571111853.